

THE 4TH INTERNATIONAL CONFERENCE ON ALUMINUM ALLOYS

THE SOLIDIFICATION BEHAVIOR OF Al-Mg ALLOYS AND THE INFLUENCE OF Cu AND Mn ADDITIONS

Y. L. Liu¹, S. B. Kang², H. K. Cho³ and Z. Q. Hu¹

1. Institute of Metal Research, Academia Sinica, Shenyang, China
2. Korea Institute of Machinery and Metals, Changwon, Korea
3. Kyungpook National University, Taegu, Korea

Abstract

The as-cast microstructure of Al-Mg alloys consisted of α -Al matrix plus eutectic structure Al_8Mg_5 under the condition of normal solidification, and it was influenced by the cooling rate. The addition of Cu promoted the segregation of Mg and resulted in the formation of nonequilibrium eutectic structure $Al_xCu_yMg_z$. The addition of small Mn has little influence on the solidification of Al-Mg alloys. The Mn atoms were trapped by constituent Al_6Fe . But, in the alloy with high level of Mn, the primary phase would become Al_6Mn , and the solidification process was relatively complicated.

Introduction

Aluminum-magnesium alloys have recently been subjected to intensive investigation [1-10] in order to improve the mechanical properties. Most of the works were on the alloy design, heat treatment, hot working, etc., and the research on solidification behavior is limited. The metallurgical factors have great influence on the mechanical and physical properties of the materials [11,12]. The solute redistribution during solidification process results in microsegregation and, often, the formation of a low melting point eutectic structure although the chemical composition is much lower than the solid solubility limit. The coarse low melting point eutectic structure would severely deteriorate the mechanical properties [13,14]. Therefore, the research on the solidification and segregation of the alloys has commercial interest.

Al-Mg alloys are non-heat treatable alloys. The mechanical properties can be improved by adding alloying elements. The addition of the elements would make the solidification process more complicated. In the present work, the influence of Cu and Mn additions on the solidification behavior of Al-Mg alloys have been studied.

Experimental Procedures

The as-received materials used in this study were homogenized ingots with the chemical compositions listed in Table I. The ingots were cast from high pure Al, Cu, Mg (99.99%) and Al-Mn (10wt%Mn) master alloy. The solidification behavior of the alloys was investigated by remelting the alloys. The specimens with the size of $10 \times 10 \times 30$ mm were cut from the homogenized ingots. The alloys were first heated to $690\text{--}700^\circ\text{C}$ in an air furnace in graphite crucible and held at the temperature for 10 min to melt that materials entirely and homogenize the composition. They were then cooled in air.

Table I The chemical compositions of the alloys (wt%)

alloys	Mg	Cu	Mn	Fe	Si	Al
I	7.12			0.08	0.09	bal.
I-1	7.18	0.45		0.07	0.08	bal.
I-2	6.80	0.97		0.06	0.07	bal.
I-3	7.57	1.45		0.06	0.08	bal.
I-4	7.39	1.78		0.07	0.08	bal.
II	8.28			0.07	0.08	bal.
II-1	8.15		0.40	0.07	0.08	bal.
II-2	7.96		1.79	0.06	0.08	bal.

The microstructure was analyzed by optical microscopy and in the electron microprobe. The specimens were prepared by standard metallographic procedures and etched by Knoll's reagent. The electron probe analysis was done with a JAX-8600 Electron Probe X-ray Microanalyzer (EPMA) at an accelerating potential of 20 kV to determine the compositions of the intermetallic phases. The size and areal fraction of the eutectic compound were measured by a LECO-200 Imaging Analysis System. The results were the average values of five fields selected randomly. The areal fraction was assumed to be equivalent to the volume fraction. The dendrite arm spacing (DAS) was measured by metallographic photos.

Results and Discussion

The Solidification Behavior of Al-Mg Alloys

Fig.1 shows the as-cast microstructures of alloy I solidified at the cooling rate of $60^\circ\text{C}/\text{min}$. It consisted of α -Al, Al_3Mg_5 as well as Al_6Fe and Mg_2Si . The α -Al with dendritic structure was the primary phase and formed the matrix of the materials, and the Al_3Mg_5 with a "Chinese script" structure was the product of eutectic reaction $L \rightarrow \alpha\text{-Al} + \text{Al}_3\text{Mg}_5$, while the Al_6Fe and Mg_2Si with a blocky structure were minor constituents. The solidification process of binary Al-Mg is relatively simple. The primary phase α -Al first precipitated from liquid, and Mg atoms were rejected into the interdendritic regions, which resulted in the increase of solute concentrations in the remaining liquid. As soon as the eutectic composition was reached in the finally solidified zone, the eutectic reaction $L \rightarrow \alpha\text{-Al} + \text{Al}_3\text{Mg}_5$ occurred and the solidification process terminated. The main solidification sequence was $L \rightarrow \alpha\text{-Al} + L_1 \rightarrow \alpha\text{-Al} + \text{Al}_3\text{Mg}_5$. With increasing the Mg content in the alloys, the volume fraction and size of eutectic structure increased remarkably. Imaging analysis showed that the volume fraction of eutectic compound Al_3Mg_5 was 3.67% in alloy I, and 4.87% in alloy II. Obviously, the microstructures of the alloys were influenced by chemical compositions.

The cooling rate is another factor affecting the solidification behavior and the as-cast microstructure. Slow cooling retarded eutectic reaction and resulted in the formation of

single phase structure. As to alloy I, when solidified at the cooling rate of 2.3°C/min, the as-cast microstructure was single phase α -Al, and no evidence of eutectic structure was observed. With increasing cooling rate to 5°C/min, the as-cast microstructure consisted of a α -Al matrix plus a little eutectic structure, and the eutectic compound Al_8Mg_5 was quite small. Alloy II had a still low cooling rate for forming single phase structure. Eutectic structure began to form in the specimen solidified at the cooling rate of 1.5°C/min. The higher the Mg content in the alloys, the lower the cooling rate for forming single phase structure. As to the high Mg alloy, for example, Al-11Mg, the critical cooling rate for forming single phase α -Al was about 1°C/min[15].

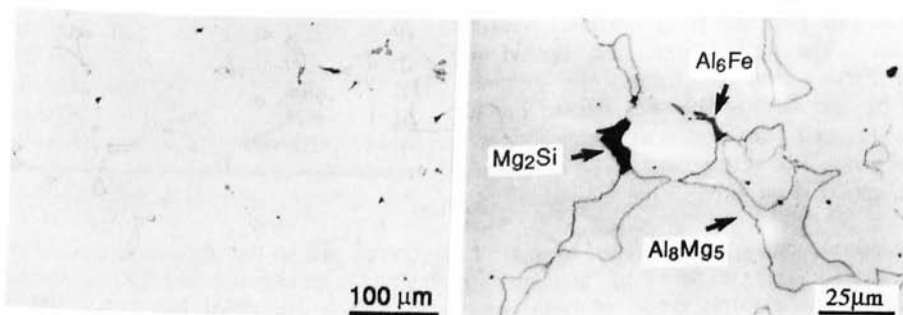


Fig.1 The microstructure of alloy I

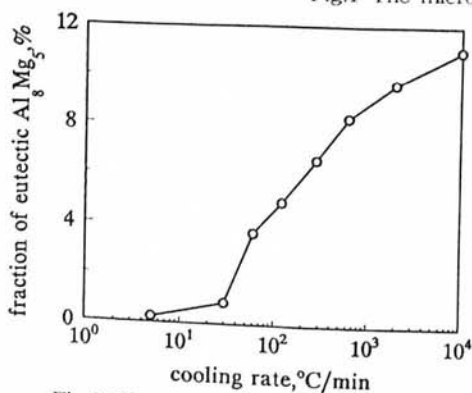


Fig.2 The fraction of eutectic compound Al_8Mg_5 vs cooling rate

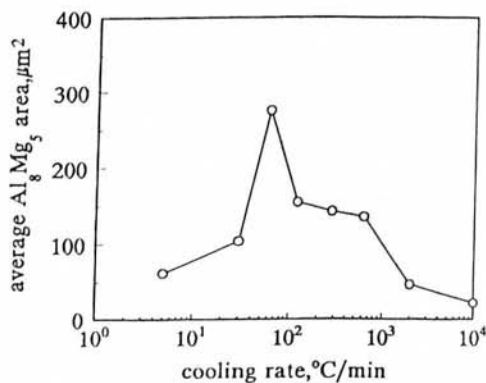


Fig.3 The size of eutectic compound Al_8Mg_5 vs cooling rate

Fig.2 and Fig.3 show the influence of cooling rate on the volume fraction and size of eutectic compound Al_8Mg_5 , respectively. With increasing cooling rate, the fraction of eutectic compound Al_8Mg_5 increased quickly. But the change tendency of eutectic size with cooling rate was different. First, the eutectic size increased with the increase of cooling rate. After reaching to a largest size, it then decreased with the further increase of cooling rate. The cooling rate for producing the largest eutectic size was located at about 60°C/min. Slow and rapid solidification all produced fine eutectic structure. The dendrite arm spacing was also a function of the cooling rate. The regression analysis through the data points of alloy I showed that the function can be represented by the following equation:

$$\text{DAS} = 417\varepsilon^{-0.32}$$

where DAS represents the dendrite arm spacing in μm , and ε represents the cooling rate in $^{\circ}\text{C}/\text{min}$.

From Al-Mg phase diagram [16], the solid solubility limit of magnesium in aluminum is about 17wt%, which is much higher than the Mg content in the alloys used in this study. In the case of equilibrium solidification, the as-cast microstructure should be single phase α -Al. Obviously, the formation of eutectic structure α -Al+Al₈Mg₅ resulted from the segregation of solute Mg. The research on the line profile of Mg concentration showed that the solute segregation was quite clear. With the precipitation of α -Al, solute Mg was rejected to the interface front and the concentration of Mg in the remaining liquid rose gradually. As soon as the eutectic composition was reached, the eutectic reaction $L \rightarrow \alpha$ -Al+Al₈Mg₅ occurred. This was consistent with the solidification path defined by Scheil model[17].

As to the alloy with a composition less than solubility limit, in the case of equilibrium solidification, the as-cast microstructure will be uniform single phase structure and no microsegregation takes place. With increasing cooling rate, the solidification model will transform gradually to nonequilibrium and the microsegregation will occur. As soon as the microsegregation reaches to a high extent that the concentration of Mg in growing α -Al reaches the solubility limit, the eutectic structure will appear in the final microstructure. In the case of normal solidification, the higher the cooling rate, the more severe the microsegregation and the easier the eutectic structure to form. The slow cooling is favorable to form single phase structure. The eutectic reaction was retarded easier in Al-Mg alloys than in Al-Li alloys[18] and Al-Mg-Cu alloys[15].

The eutectic size was influenced by both eutectic fraction and grain size. In general, with the reduction of cooling rate, the grain size increases, and the finally solidified zone is localized, which results in the increase of the size of finally solidified zone. As a result, the eutectic reaction occurs in the minority regions and the eutectic structure possesses larger size. On the other hand, in the case of low cooling rate, with the increase of cooling rate, the as-cast structure will become α -Al matrix plus eutectic α -Al+Al₈Mg₅, and the eutectic fraction increases gradually, hence, the eutectic size increases. Obviously, there exists a critical cooling rate to become the largest eutectic. As to Al-Mg alloys, it was about 60 $^{\circ}\text{C}/\text{min}$.

The Influence of Cu Addition

The addition of Cu resulted in the formation of relatively complicated microstructure. In the as-cast specimens solidified with a cooling rate of 60 $^{\circ}\text{C}/\text{min}$, five phases of α -Al, Al_xCu_yMg_z, Al₈Mg₅, Al₆Fe and Mg₂Si were observed, as shown in Fig.4. Al_xCu_yMg_z was a product of nonequilibrium eutectic reaction and possessed lamellar structure. The electron microprobe analysis showed that its composition was very different from the equilibrium compounds Al₂MgCu and Al₆Mg₄Cu found in Al-Mg-Cu alloys [19]. Therefore, its constitution was defined as Al_xCu_yMg_z for the present. The Al₈Mg₅ was usually observed at the edge of Al_xCu_yMg_z, but, its fraction was reduced remarkably, Al₆Fe and Mg₂Si were the minor constituents, same as in the alloy I.

The content of Cu has great influence on the Al_xCu_yMg_z. Fig. 4 shows that with the

increase of Cu content, the size and the fraction of $Al_xCu_yMg_z$ rose, while the lamellar spacing reduced. The imaging analysis showed that the fraction of $Al_xCu_yMg_z$ in alloy I-1 was 4.85% while in alloy I-3, got up to 9.28%. The concentration analysis by EPMA showed that the composition of $Al_xCu_yMg_z$ in the four alloys were also different. Increasing Cu content gave rise to the rising of Cu concentration in the $Al_xCu_yMg_z$, as shown in Table II. The solidification process of the alloys with Cu addition is very different from the Al-Mg binary alloys. With the temperature dropping, the reaction $L \rightarrow L' + \alpha-Al$ is also the main event during solidification. As the primary $\alpha-Al$ precipitated from the liquid and the solid-liquid interface advanced forward, the solute atoms Cu and Mg with redistribution coefficient less than unity enriched at the interface front. As soon as the solubility limit of the solute in growing $\alpha-Al$ was reached, a new phase would form from the remaining liquid. Solidification theory [20] predicts that the final structure consists of $\alpha-Al$, Al_6Mg_4Cu and Al_8Mg_5 . The $\alpha-Al$ first precipitates from liquid, then the binary eutectic $\alpha-Al + Al_6Mg_4Cu$ follows, and finally, the ternary eutectic reaction $L \rightarrow \alpha-Al + Al_6Mg_4Cu + Al_8Mg_5$ occurs in the finally solidified zone. But EPMA showed that the composition of the Cu-containing compound in the final structure was very different from that of Al_6Mg_4Cu . It was the result of nonequilibrium eutectic reaction. Relatively large cooling rate and diffusion difficulty in solid resulted in that $Al_xCu_yMg_z$ would not reach the nominal composition of Al_6Mg_4Cu .

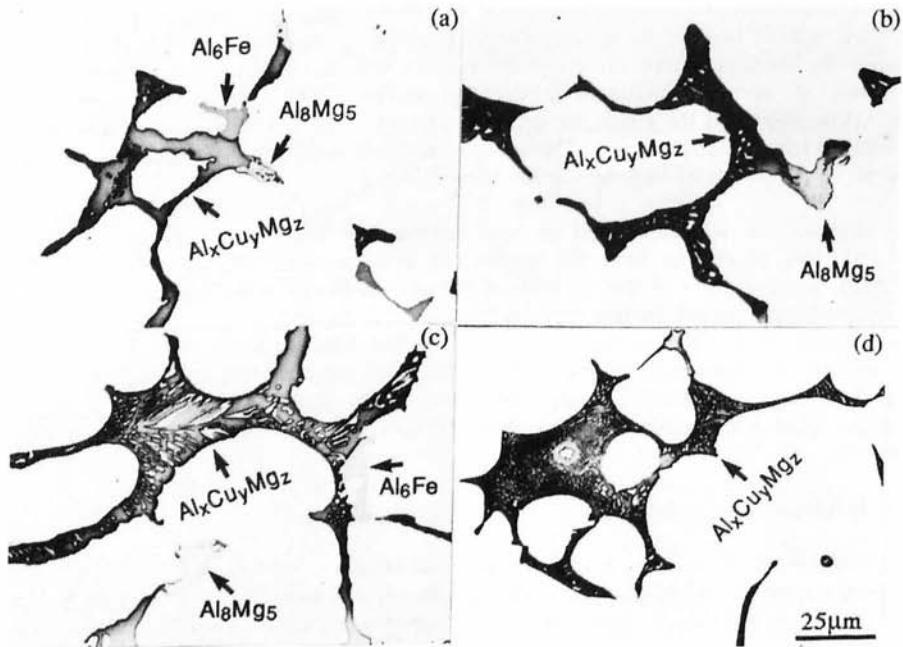


Fig.4 The microstructures of alloy I-1 (a), alloy I-2 (b), alloy I-3 (c) and alloy I-4 (d)

With the increase of the contents of Cu in the alloys, the segregation tendency increased. The Cu atoms segregated to the interdendritic regions increased, hence, the Cu concentration of remaining liquid at interdendritic regions rose. When the nonequilibrium eutectic reaction took place, the $Al_xCu_yMg_z$ would have higher concentration of Cu. In alloy I-4, the Cu

concentration of $Al_xCu_yMg_z$ reached 23.16 wt%, which was higher than that of Al_6Mg_4Cu (22.48wt%).

On the other hand, the addition of Cu promoted the segregation of Mg atoms. With increasing Cu content, the redistribution coefficient of solute Mg reduced, which resulted in the rising of Mg segregation. More Mg atoms would segregate to interdendritic regions, and the finally solidified zone increased, which gave rise to the increase of the fraction of $Al_xCu_yMg_z$ in the final microstructure.

Table II The compositions of $Al_xCu_yMg_z$ (wt%)

alloy	Al	Mg	Cu
I-1	56.10	30.81	12.71
I-2	52.34	28.94	18.47
I-3	48.70	30.31	20.62
I-4	46.94	29.36	23.16

The Influence of Mn Addition

Fig. 5 and Fig. 6 show the as-cast microstructures of the alloys with Mn additions solidified at the cooling rate of 60°C/min. Alloy II-1 was quite simple and similar to binary Al-Mg alloys. In addition to the primary phase α -Al, the eutectic compound Al_8Mg_5 and minor constituent Mg_2Si , there was a minor constituent $Al_6(MnFe)$. With the increase of Mn in alloys, the microstructures of the alloys become more complicated. In alloy II-2, the primary phase was Al_6Mn with block or "Chinese script" structure, see Fig.7. The matrix α -Al was the product of eutectic reaction $L \rightarrow \alpha-Al + Al_6Mn$. At the grain boundary and interdendrite, the microstructure consisted of Al_8Mg_5 , Mg_2Si and plate-like Al_6Mn , while blocky $Al_6(MnFe)$ no longer appeared.

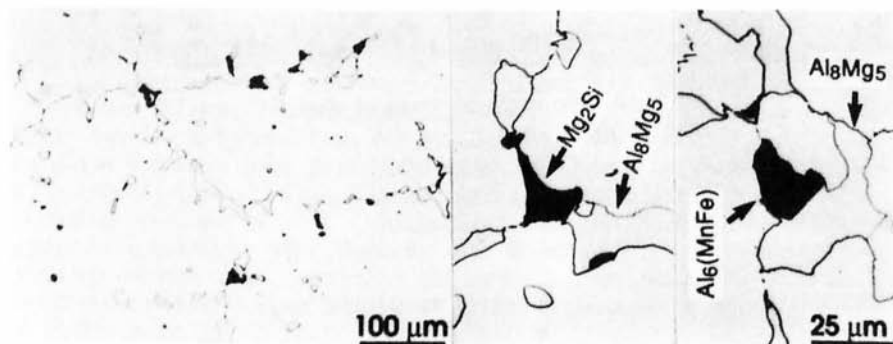


Fig.5 The microstructure of alloy II-1

In alloy with low Mn, the influence of Mn on the solidification behavior was not great. The solidification path was similar to the binary Al-Mg system. The only difference was that insoluble constituent Al_6Fe transformed $Al_6(MnFe)$. The Mn atoms were trapped by Al_6Fe and replaced some Fe atoms of Al_6Fe . With the increase of Mn content, in alloy II-2, the initial solidification reaction was $L \rightarrow Al_6Mn + L'$. When the eutectic composition was reached at the solid-liquid interface front, eutectic reaction $L \rightarrow \alpha-Al + Al_6Mn$ took place. The eutectic compound Al_6Mn continued to grow on the primary Al_6Mn . The α -Al with dendritic structure formed the matrix of the material. The precipitation of Al_6Mn consumed the Mn

atoms, the Mn atom depletion occurred in the unsolidified zone. Therefore, the local composition of remaining liquid would shift back toward L+ α -Al region. As the α -Al precipitated, the Mn atoms re-enriched in the finally solidified zone. As soon as the solid solubility limit of Mn in α -Al was reached, the eutectic-like reaction L \rightarrow α -Al+Al₆Mn occurred, and the Al₆Mn displayed plate-like structure. Then, the remaining liquid shifted back toward L+ α -Al phase region again, and the Mg atoms continued to enrich in the interface front. Finally, as the solid solubility of Mg in growing α -Al was reached, the eutectic reaction L \rightarrow α -Al+Al₈Mg₅ occurred and terminated the solidification process. Since the precipitation of Al₆Mn did not consume Mg atoms, the fraction of the eutectic compound Al₈Mg₅ was not affected by the Mn addition. Obviously, the influence of Mn addition on the solidification behavior of Al-Mg alloys was different from that of Cu addition. The solidification sequence of alloy II-2 was summarized as L \rightarrow Al₆Mn+L₁ \rightarrow Al₆Mn+ α -Al+L₂ \rightarrow Al₆Mn+ α -Al+plate-like Al₆Mn+L₃ \rightarrow Al₆Mn+ α -Al+plate-like Al₆Mn+Al₈Mg₅.

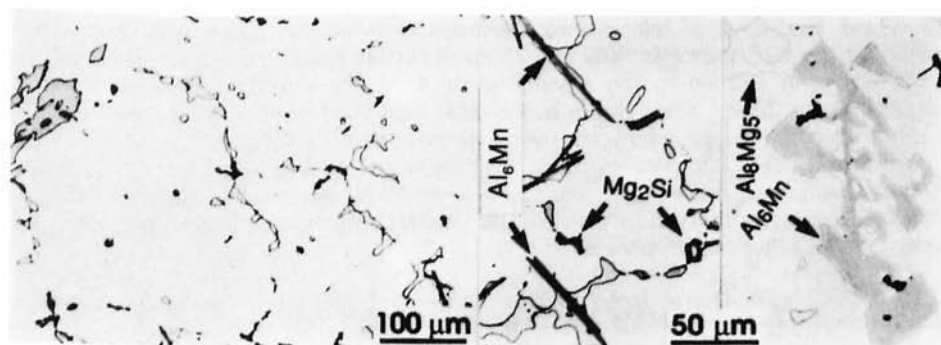


Fig.6 The microstructures of alloy II-2

Fig.7 The primary phase Al₆Mn in alloy II-2

Conclusions

- 1) Binary Al-Mg alloy exhibited a relatively simple solidification behavior, with a phase transformation path $L \rightarrow \alpha\text{-Al}+L_1 \rightarrow \alpha\text{-Al}+\text{Al}_6\text{Mg}_5$. The volume fraction and size of eutectic structure were influenced by alloy composition.
- 2) Cooling rate was an important factor affecting solidification behavior. Slow cooling retarded the occurring of eutectic reaction and resulted in the formation of single phase $\alpha\text{-Al}$. With increasing cooling rate, the volume fraction of eutectic structure increased correspondingly. But, the size of eutectic structure reached a maximum value at about 60°C/min, both slow and rapid cooling gave rise to the reduction of size of eutectic structure.
- 3) The addition of Cu promoted the segregation of Mg and made the solidification behavior more complicated. The solidification sequence of Cu-containing Al-Mg alloys became $L \rightarrow \alpha\text{-Al}+L_1 \rightarrow \alpha\text{-Al}+\text{Al}_x\text{Cu}_y\text{Mg}_z+L_2 \rightarrow \alpha\text{-Al}+\text{Al}_x\text{Cu}_y\text{Mg}_z+\text{Al}_6\text{Mg}_5$.
- 4) The addition of small Mn had little influence on the solidification behavior of Al-Mg alloys. Mn atoms were trapped by Al_6Fe and constitution Al_6Fe transformed into $\text{Al}_6(\text{MnFe})$. With increasing the Mn content, Al_6Mn would precipitate as primary phase. The solidification sequence of alloy II-2 was $L \rightarrow \text{Al}_6\text{Mn}+L_1 \rightarrow \text{Al}_6\text{Mn}+\alpha\text{-Al}+L_2 \rightarrow \text{Al}_6\text{Mn}+\alpha\text{-Al}+\text{plate-like } \text{Al}_6\text{Mn}+L_3 \rightarrow \text{Al}_6\text{Mn}+\alpha\text{-Al}+\text{plate-like } \text{Al}_6\text{Mn}+\text{Al}_6\text{Mg}_5$.

References

- [1] Y. L. Liu and S.B. Kang, submitted to "Metall. Trans."
- [2] T.Murakami, M. Yamamoto, A.Kanio and T.Takahashi, J.Jpn. Inst.Light Met., 40,(1990),538
- [3] T. R. McNelley, E. W. Lee and M. E. Mills, Metall. Trans., 17A,(1986),1035
- [4] E.W.Lee,T.R. McNelley and A.F.Stengel, Metall. Trans., 17A,(1986),1043
- [5] T.Daitoh and T.Takaai, J.Jpn.Inst.Light Met.,39,(1989),837
- [6] Sheng-Long Lee and Shinn-Tyan Wu, Metall. Trans., 17A,(1986),833
- [7] Zhaoqi Lin and Jiaren Jiang, Acta Metall. Sinica (in Chinese), 24. Suppl. I.,(1988),54
- [8] M.Yanagawa,M.Abe and S.Ohie, R.D.Kobe Steel Engineering Reports, 43,(1993),97
- [9] G.Itoh,B.Cottureau and M.Kanno, J.Jpn.Inst.Light Met.,40,(1990),36,(1991),1-99, Special Issue on the Aluminum Alloy Sheets for Auto Bodies.
- [10] Hiroshige Hosomi et al., Sumitomo Light Metal Technical Reports,32, No.1,
- [11] G. T. Hahn and A. R. Rosenfield, Metall. Trans., 6, (1975),653
- [12] D. S. Thompson, Metall. Trans., 6, (1975),671
- [13] H. W. Antes and S. Lipson, Trans. TMS-AIME, 239, (1967),1634
- [14] S. N. Singh and M. C. Flemings, Trans. TMS-AIME, 245, (1969),1811
- [15] Y. L. Liu and S. B. Kang, to be published
- [16] L. F.Mondolf, Aluminum Alloys, Structure and Properties(Butterworth & Co (Publisher) Ltd, 1976), 312
- [17] M. C. Flemings, Solidification Process (New York, McGraw-Hill Book Co., 1974), 31
- [18] Y. L. Liu, Z. Q. Hu et al., Metall. Trans., 24B, (1993), 857
- [19] L. F.Mondolf, Aluminum Alloys, Structure and Properties (Butterworth & Co (Publisher) Ltd, 1976), 498
- [20] M. C. Flemings, Solidification Process (New York, McGraw-Hill Book Co., 1974), 188